IEEE Access
Multidisciplinary | Rapid Review | Open Access Journal

SPECIAL SECTION ON PHYSICAL AND MEDIUM ACCESS CONTROL LAYER ADVANCES IN 5G WIRELESS NETWORKS

Received January 22, 2017, accepted February 26, 2017, date of publication May 2, 2017, date of current version July 7, 2017.

Digital Object Identifier 10.1109/ACCESS.2017.2696822

INVITED PAPER

Energy and Traffic Aware Full-Duplex Communications for 5G Systems

ANIMESH YADAV[1], (Member, IEEE), OCTAVIA A. DOBRE[1], (Senior Member, IEEE), AND NIRWAN ANSARI[2], (Fellow, IEEE)

[1]Faculty of Engineering and Applied Science, Memorial University, St. John's, NL A1B 3X5, Canada
[2]Department of Electrical and Computer Engineering, New Jersey Institute of Technology, Newark, NJ 07102, USA

Corresponding author: Animesh Yadav (animeshy@mun.ca)

ABSTRACT In this paper, we consider the problem of resource allocation in a dense small-cell network. Each small-cell base station is powered by a renewable energy source and operates in the full-duplex mode. We account for the rate-dependent energy term for data decoding into the total energy consumption at the small-cell base station. Owing to this new energy term, the transmitter and receiver operations now draw the energy from a common source. For a new energy consumption model and high interference scenario, which arises due to full-duplex communications, we formulate an energy and load aware resource management optimization problem under the energy causality and total transmit power constraints of the small-cell base station and uplink user equipments. In particular, the problem minimizes the data queue length of each network user equipment by jointly designing the beamformers, power, and sub-carrier allocation and their scheduling. Owing to the non-convexity of the problem, a global solution is inefficient; thus, we opt for the successive parametric convex approximation method to obtain a sub-optimal solution. This method solves for the convex approximate of the non-convex problem in each iteration and leads to faster convergence. For practical implementation, we further develop a distributed algorithm by using the dual decomposition framework, which relies on limited exchange of information between the involved base stations. Numerical simulations compare the network scenario which accounts for uplink channel rate-dependent energy consumption with that which ignores it. Results advocate the need for redesigning of the resource allocation scheme. In addition, numerical simulations also validate the usefulness of full-duplex communications over the half-duplex communications in terms of minimizing the sum data queue length of the users.

INDEX TERMS 5G, small cells, full-duplex communications, energy harvesting communications, rate-dependent decoding energy, successive parametric convex approximation, radio resource management.

I. INTRODUCTION

The future generation of mobile communications is envisioned to provide a 1000-fold increase in data rate and enhanced user experience. In this respect, the fifth generation (5G) radio access technology is engineered to provide a total solution to satisfy a wider range of network requirements for 2020 and beyond. Dense deployment of small cells is predicted to be one of the key technologies to achieve humongous data rate promised by the 5G cellular network standard [1]. Small cells increase the throughput and user experience by bringing the base stations closer to the users, especially in high-traffic areas. Furthermore, small cells are low power, low cost and easy to deploy without much planning as compared to macro cells.

Owing to arbitrary and dense deployment, not all small cell base stations (SBSs) have the privilege to draw power from the grid source. Thus, alternatively, energy harvested from nature is a viable source to power the majority of them [2]. The clear contribution of using harvested energy is reduced CO_2 emission into the environment [3]. Energy can be harvested from nature using solar and wind sources. Although such sources provide a greener environment, the energy casualty and randomness in arrival leaves the SBS sometimes inactive, thus incurring service interruption [4].

In order to shorten the transceiver inactive state due to the unavailability of energy, numerous works reconsider the communication system design and techniques when powered by an intermittent source of energy [5]–[11].

Simultaneous transmission and reception of signals on the same time-frequency resource, i.e., full-duplex (FD) communications, is another technique to improve the spectral efficiency of the network. Although this technique has been known, it has not been used due to hardware incapability to handle self-interference (SI) [12]. SI arises due to the high power transmit signal listened by the collocated receiver, and thus diminishes the intended low power received signal. Recently, efforts have been made to cancel SI in both analog and digital domains jointly, e.g., [13]–[15], such that FD communications becomes a reality. These works essentially validate the applicability of FD communications for a short distance, where the transceiver transmits with lower power. Thus, the FD transceiver has been considered for small cells, which have a short range of operation [16]–[18]. Furthermore, since the small cells have a range of operation of approximately 100 meters, the energy spent in decoding the received data is non-negligible [19], [20]. Hence, recent works [10], [11], [21], [22] accounted for the received data rate-dependent decoding energy (DE) in their problems for a more realistic formulation. DE is required to process the received data that are protected by some outer code, such as turbo or low-density parity check codes.

At the network level, FD communications receives interference from both within the cell and neighboring cells, which is significant. Recently, a few works [17], [23]–[25] studied the increase due to the inter-cell interference where the base station in each cell is deployed with an FD transceiver. Goyal *et al.* [17] explored the problem of user selection and power allocation to efficiently mitigate the excessive interference. Mungara and Lozano [23] studied the interference surge due to FD communications and characterized the actual increase in system spectral efficiency via stocastic geometry. Cirik*et al.* [24] considered FD SBSs and user equipments (UEs), and proposed the transmit and receiver beamformer design by maximizing the system sum rate. Chen *et al.* [25] considered the energy harvesting SBSs and to eliminate both the inter- and intra-cell interference, they proposed transmit and receive beamformers under the energy causality constraint. However, none of these works accounted for the fact that a non-negligible amount of energy comparable to the transmit energy of the SBSs is consumed in the decoding operation of the received signal. Hence, by accounting for the DE term in the total energy consumption expression at the SBSs makes the system model practical and appropriate.Owing to this newly introduced term, the available harvested energy at the SBS is now shared among the transmitter and receiver operations, unlike its previous use only for the transmitter operations. Optimal energy sharing, on the other hand, depends on the downlink (DL) and uplink (UL) channel conditions. Besides, the data rates achieved by the UL UEs are dependent on the available energy at the SBS as well. Hence, the solutions obtained in all previous works are not any more applicable in this scenario.

In this paper, we consider a two-tier heterogeneous network (HetNet) consisting of a macro cell and many small cells. In the small cell tier, all SBSs operate in the FD mode and serve simultaneously multiple DL and UL UEs. Since the wireless traffic is non-uniform, each UE has a different amount of data in its buffer to be transmitted. Hence, minimizing the data queue length of the UEs is an appropriate objective for network operators as it tends to avoid the excessive resource allocation. With the goal of efficiently managing the network resources in an excessive surge of interference due to FD communications, we formulate a problem to jointly design the transmit beamformer, power and sub-carrier allocation, and UEs scheduling. The problem minimizes the length of the data queue of each UE, under the energy casualty and total transmit energy constraint. The energy casualty constraint ensures that the amount of energy used by the SBSs does not exceed the amount of energy harvested. The distinct features of this paper are summarized as follows:

- We consider a realistic scenario of densely deployed FD small cells that are powered by energy harvesting (EH) source, as all SBSs cannot be powered by grid source. We also account for the received data rate-dependent DE into the power consumption model. Then, a novel optimization problem is formulated that minimizes the data queue length of UEs for the joint design of transmit beamformers and power allocation under the SBS energy casualty constraint. The solution implicitly provides the sub-carrier allocation and UEs scheduling.
- The formulated problem is non-convex and solving it optimally is computationally intractable. Hence, we transform and approximate the original problem into a tractable and convex form, respectively. Then, we solve the convex approximated problem by using the successive parametric convex approximation (SPCA) framework [26] and propose a centralized algorithm.
- For practical applicability, we further propose a distributed algorithm by using the framework of dual decomposition, where the convex approximated problem is decomposed into multiple independent subproblems corresponding to each active base station (BS), which can hence be solved locally with minimum information exchange.

The rest of the paper is organized as follows. Section II introduces the system model and formulates the optimization problem. Section III develops a low-complexity centralized algorithm based on the SPCA framework to solve the formulated optimization problem. Section IV discusses the development of a distributed algorithm for the formulated optimization problem. Section V presents numerical results and discussions. Finally, conclusion of the paper is given in Section VI.

Nomenclature: We use bold uppercase letters to denote matrices and bold lowercase letters to denote vectors.

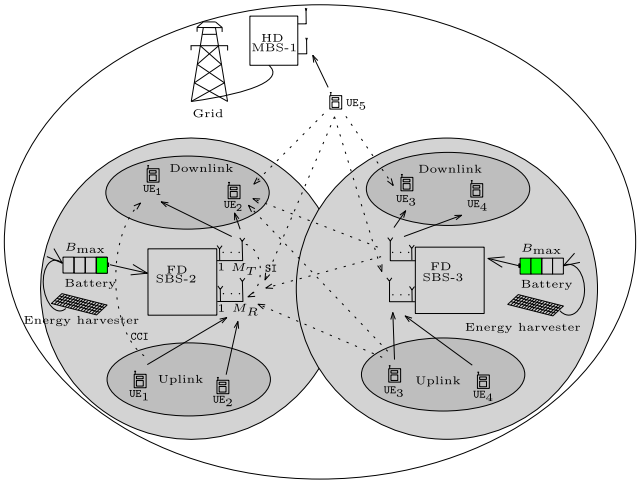

FIGURE 1. A typical network depiction with multiple FD SBSs serving multiple DL and UL UEs and a HD MBS is operating in UL mode.

$(x)^H$ and $(x)^T$ stand for the Hermitian and transpose operation on x, respectively. $|x|$ represents the absolute of $x \in \mathcal{C}$, while $||x||_2$ is the ℓ_2-norm of x. tr$\{\cdot\}$ and $\mathbb{E}\{\cdot\}$ denote the trace and expectation operators, respectively. $\mathbf{I}_L$ denotes the $L \times L$ dimension identity matrix.

II. SYSTEM MODEL AND PROBLEM FORMULATION

A. SYSTEM MODEL

We consider a two-tier multi-carrier HetNet consisting of one half-duplex (HD) macro base station (MBS) and B EH FD SBSs in the macrocell and small cell tiers, respectively, serving a few HD UEs. The total system spectrum is shared among the two tiers in the network. Each SBS is installed with a rechargeable battery and an EH device, which are used to store and collect the harvested energy, respectively. The MBS is equipped with M antennas, whereas SBSs are equipped with $M_T + M_R$ antennas, of which M_T antennas are used to transmit data on the DL channel and M_R antennas are used to receive data on the UL channel, as shown in Fig. 1. Each base station b, including SBSs and MBS, belongs to a set denoted by $\mathcal{B} = \{1, \ldots, B+1\}$. The sets of all DL and UL UEs are denoted by $\mathcal{D} = \{1, \ldots, K_{\mathrm{D}}\}$ and $\mathcal{U} = \{1, \ldots, K_{\mathrm{U}}\}$, respectively. We assume that data for the DL UE i are transmitted only from one SBS, and are denoted by $b_i \in \mathcal{B}$. Similarly, the data of UL UE j are processed by only one SBS, and are denoted by $b_j \in \mathcal{B}$.[1] The sets of all DL and UL UEs associated to SBS b are denoted by $\mathcal{D}_b \in \mathcal{D}$ and $\mathcal{U}_b \in \mathcal{U}$, respectively. The SBSs send and receive data simultaneously to K_{D} UEs on the DL channels and from K_{U} UEs on the UL channels, respectively. We further assume that the MBS is serving the UEs on the UL channels. A total of N equal bandwidth sub-channels belonging to the set $\mathcal{N} = \{1, \ldots, N\}$ are available in the system.

[1]For clarity, considering Fig. 1, for DL UEs $i = \{1, 2, 3, 4\}$, the serving BS for UEs $\{1, 2\}$ is $b = b_1 = b_2 = 2$ and for UEs $\{3, 4\}$ is $b = b_3 = b_4 = 3$. Similarly, for UL UEs $j = \{1, \ldots, 5\}$, the serving BS for UEs $\{1, 2\}$ is $b = b_1 = b_2 = 2$ and so on.

The received signal over sub-channel n at DL UE i is given by

$$y^{\mathrm{D}}_{i,n} = \mathbf{h}^H_{b_i,i,n}\mathbf{w}_{i,n}s^{\mathrm{D}}_{i,n} + \underbrace{\sum_{k\neq i}^{K_{\mathrm{D}}} \mathbf{h}^H_{b_k,i,n}\mathbf{w}_{k,n}s^{\mathrm{D}}_{k,n}}_{\text{MUI + CCI due to all DL UEs}} + \underbrace{\sum_{j=1}^{K_{\mathrm{U}}} g_{j,i,n}\sqrt{p_{j,n}}s^{\mathrm{U}}_{j,n}}_{\text{CCI due to all UL UEs}} + n^{\mathrm{D}}_{i,n}, \quad (1)$$

where $\mathbf{w}_{i,n}$ and $p_{j,n}$ are the beamforming vector and power coefficient corresponding to the DL and UL UEs i and j, respectively, on sub-channel n. $\mathbf{h}_{b_i,i,n} \in \mathbb{C}^{M_T \times 1}$ is the channel vector from SBS b_i to DL UE i and $g_{j,i,n}$ is the complex channel coefficient from UL UE j to DL UE i on the sub-channel n. Each channel coefficient includes path loss and small-scale fading components. $s^{\mathrm{D}}_{i,n}$ and $s^{\mathrm{U}}_{j,n}$ are the unit energy data symbol corresponding to the DL and UL UEs, respectively. The term $n^{\mathrm{D}}_{i,n} \sim \mathcal{CN}(0, \sigma_n^2)$ is the additive white Gaussian noise (AWGN). In (1), the first and second terms on the right-hand side represent the intended signal, and the aggregate of intra-cell multiuser interference (MUI) and inter-cell co-channel interference (CCI) due to all DL transmissions, respectively. The third term represents the CCI due to all UL transmissions. The received signal-to-interference plus noise ratio (SINR) of DL UE i over sub-channel n can be written as

$$\gamma^{\mathrm{D}}_{i,n} = \frac{\mathbf{h}^H_{b_i,i,n}\mathbf{W}_{i,n}\mathbf{h}_{b_i,i,n}}{\sigma_n^2 + \sum_{k\neq i}^{K_{\mathrm{D}}} \mathbf{h}^H_{b_k,i,n}\mathbf{W}_{k,n}\mathbf{h}^H_{b_k,i,n} + \sum_{j=1}^{K_{\mathrm{U}}} p_{j,n}|g_{j,i,n}|^2}, \quad (2)$$

where $\mathbf{W}_{i,n} = \mathbf{w}_{i,n}\mathbf{w}^H_{i,n}$ is a positive semi-definite (PSD) matrix.

Next, for the UL transmission, the received signal vector of UE j over sub-channel n at base station b_j is given by

$$\mathbf{y}^{\mathrm{U}}_{j,n} = \mathbf{h}_{b_j,j,n}\sqrt{p_{j,n}}s^{\mathrm{U}}_{j,n} + \sum_{l\neq j}^{K_{\mathrm{U}}} \mathbf{h}_{b_j,l,n}\sqrt{p_{l,n}}s^{\mathrm{U}}_{l,n} + \underbrace{\sum_{i=1}^{K_{\mathrm{D}}} \mathbf{H}_{b_j,b_i,n}\mathbf{w}_{i,n}s^{\mathrm{D}}_{i,n}}_{\text{SI + CCI from all DL UEs}} + \mathbf{n}^{\mathrm{U}}_{j,n}, \quad (3)$$

where $\mathbf{h}_{b_j,j,n} \in \mathbb{C}^{M_R \times 1}$ is the channel vector from UL UE j to SBS b_j and $\mathbf{n}^{\mathrm{U}}_{j,n} \sim \mathcal{CN}(0, \sigma_n^2\mathbf{I}_{M_R})$ is the AWGN noise vector. In (3), the first right-hand side term is the intended signal. The second right-hand side term represents the intra-cell multiple access interference and inter-cell CCI due to all UL transmissions. The third term represents the total CCI due to inter-cell DL transmissions including SI, where $\mathbf{H}_{b_j,b_i,n}$ is the channel matrix from SBS b_j to SBS b_i. In order to recover each UL UE data, we treat the SI and CCI as background noise and apply the minimum mean square error (MMSE) successive interference cancellation receiver. Then,

the received SINR of UL UE j over sub-channel n is given by

$$\gamma_{j,n}^{\mathrm{U}} = p_{j,n}\mathbf{h}_{b_j,j,n}^{H}\Bigg(\sigma_n^2\mathbf{I}_{M_R} + \sum_{l>j}^{K_{\mathrm{U}}} p_{l,n}\mathbf{h}_{b_j,l,n}\mathbf{h}_{b_j,l,n}^{H} + \sum_{i=1}^{K_{\mathrm{D}}} \mathbf{H}_{b_j,b_i,n}\mathbf{W}_{i,n}\mathbf{H}_{b_j,b_i,n}^{H}\Bigg)^{-1}\mathbf{h}_{b_j,j,n}. \quad (4)$$

Let Q_i^{D} denote the number of backlogged bits assigned for DL UE i at the beginning of a given scheduling period. At that instant, the number of bits by which the backlogged bits can be reduced is given by

$$q_i^{\mathrm{D}} = Q_i^{\mathrm{D}} - \sum_{n=1}^{N}\log_2(1+\gamma_{i,n}^{\mathrm{D}}), \quad (5)$$

where the second right-hand side term is the transmission rate achieved by DL UE i. Similarly, on the UL channel, the number of bits by which the backlogged bits for UL UE j can be reduced is given by

$$q_j^{\mathrm{U}} = Q_j^{\mathrm{U}} - \sum_{n=1}^{N}\log_2(1+\gamma_{j,n}^{\mathrm{U}}), \quad (6)$$

where Q_j^{U} denotes the number of backlogged bits corresponding to UL UE j and the second right-hand side term represents the number of transmitted bits by UL UE j.

B. ENERGY ARRIVAL AND CONSUMPTION MODEL

We consider a generic energy arrival process, which is independent of the type of renewable energy source and method, at each SBS. The maximum storage size of the rechargeable battery is denoted by $B_{\max}$, which is same for all SBSs. At an SBS b, the battery is used to store the energy harvested, i.e., $TP_{b,\mathrm{H}}$ over the scheduling period T as well as the leftover energy $TP_{b,\mathrm{B}}$ from the previous period; hence, $B_{\max} \gg TP_{b,\mathrm{H}}$. We assume that the SBS knows the exact amount of energy available in the battery before the beginning of the next scheduling period. Hence, for a given scheduling period, the energy available at the SBS b is given as:

$$TP_b = \min\{B_{\max}, TP_{b,\mathrm{H}} + TP_{b,\mathrm{B}}\}, \quad (7)$$

where the $\min(\cdot,\cdot)$ operator ensures the constraint on the maximum battery size.

In short distance communications, the energies consumed in the circuit and decoding become comparable or even dominate the actual transmit power [19], [20]. Hence, it is important to include them into the total power consumption, especially when the energy comes from a renewable source. Consequently, the transmitter and receiver operations, and circuitry draw their energies from a common source that is available at the SBS; thus, the total power consumption is expressed as:

$$P_{\mathrm{tot},b} = \sum_{n=1}^{N}\sum_{i\in\mathcal{D}_b}\mathrm{tr}(\mathbf{W}_{i,n}) + P_b^{\mathrm{cir}} + \sum_{n=1}^{N}\sum_{j\in\mathcal{U}_b} P_{j,n}^{\mathrm{dec}}(R_{j,n}), \quad (8)$$

where $P_b^{\mathrm{cir}} = M_T P_{\mathrm{rf}} + P_{\mathrm{st}}$ is the total circuit power consumption, in which P_{rf} and P_{st} correspond to the active radio frequency blocks, and to the cooling and power supply, respectively. $P_{j,n}^{\mathrm{dec}}$ is the power consumption for decoding UL UE j in sub-carrier n, where $R_{j,n} = \log_2(1+\gamma_{j,n}^{\mathrm{U}})$ is the achievable rate of the UE. It should be noted that the decoding power consumption is a function of the data rate of the UE: for example, for an UL UE j, $P_{j,n}^{\mathrm{dec}}(R_{j,n}) = \alpha_j R_{j,n}$ where α_j models the decoder efficiency, being decoder specific [21], [27].

C. OPTIMIZATION PROBLEM FORMULATION

In this paper, we jointly design the beamforming vectors and power coefficients for the DL and UL UEs, respectively, such that the total number of backlogged bits in the system is minimized. In particular, we minimize the ℓ_2-norm of the deviation metrics given in (5) and (6). The main reason for using the ℓ_2-norm in the objective function is that it gives priority to the UE with a large queued data in the buffer [28].

Now, by denoting $\mathbf{W} = \{\mathbf{W}_1, \ldots, \mathbf{W}_{B+1}\}$, where $\mathbf{W}_b = [\mathbf{W}_{\mathcal{D}_b(1),1}, \ldots, \mathbf{W}_{\mathcal{D}_b(|\mathcal{D}_b|),N}]$ and $\mathbf{p} = \{\mathbf{p}_1, \ldots, \mathbf{p}_{B+1}\}$, where $\mathbf{p}_b = [p_{\mathcal{U}_b(1),1}, \ldots, p_{\mathcal{U}_b(|\mathcal{U}_b|),N}]$, the optimization problem to be solved at the beginning of each scheduling period is formulated as

$$\min_{\mathbf{W},\mathbf{p}} \ \|\mathbf{q}_{\mathrm{D}}\|_2 + \|\mathbf{q}_{\mathrm{U}}\|_2 \quad (9a)$$

$$\text{s.t.} \ \sum_{n=1}^{N}\sum_{i\in\mathcal{D}_b}\mathrm{tr}(\mathbf{W}_{i,n}) \le P_{b,\max} \quad \forall b, \quad (9b)$$

$$P_{\mathrm{tot},b} \le P_b \quad \forall b, \quad (9c)$$

$$\sum_{n=1}^{N} p_{j,n} \le P_{u,\max} \quad \forall j \in \mathcal{U}, \quad (9d)$$

$$\mathrm{rank}(\mathbf{W}_{i,n}) = 1 \quad \forall i \in \mathcal{D}, \ \forall n, \quad (9e)$$

$$\mathbf{W}_{i,n} \succeq 0 \quad \forall i \in \mathcal{D}, \ \forall n, \quad (9f)$$

$$p_{j,n} \ge 0 \quad \forall j \in \mathcal{U}, \ \forall n, \quad (9g)$$

where $\mathbf{q}_{\mathrm{D}}$ and $\mathbf{q}_{\mathrm{U}}$ have the elements $q_i^{\mathrm{D}}, i \in \{1, \ldots, K_{\mathrm{D}}\}$ and $q_j^{\mathrm{U}}, j \in \{1, \ldots, K_{\mathrm{U}}\}$, respectively. $P_{b,\max}$ is the bth SBS maximum total transmit power constraint on the DL channel, and $P_{u,\max}$ is the individual UE transmit power constraint on the UL channel. It is worth noting that (9)[2] implicitly solves the problem of sub-carrier allocation and UE scheduling as well. Hence, the optimization problem jointly designs the beamformers, power and sub-carrier allocation and UE scheduling. An UE is scheduled whenever it is allocated a non-zero power on a sub-carrier; otherwise, it is not.

In (9), the objective function (9a) ensures avoidance of the redundant resource allocation, which is limited by the data queue length of the UEs. Further, constraint (9b) ensures that the maximum transmit power allowed by SBS b for the DL transmission is limited by $P_{b,\max}$. Constraint (9c) ensures the energy causality constraint, i.e., the bth SBS total power consumption should not exceed the harvested amount. In general,

[2]Note that (9) represents equations (9a)-(9g). A similar notation is employed throughout the paper.

it is difficult to solve the above optimization problem due to the rank-one constraint (9e). Hence, we relax this constraint and proceed with the relaxed problem, which is expressed as

$$\underset{\mathbf{W},\mathbf{p}}{\text{minimize}} \ \|\mathbf{q}_{\text{D}}\|_2 + \|\mathbf{q}_{\text{U}}\|_2 \tag{10a}$$

$$\text{s.t.} \quad (9\text{b}) - (9\text{d}), (9\text{f}), (9\text{g}). \tag{10b}$$

Then, we apply a few equivalent transformations to further increase the tractability.

III. PROPOSED ALGORITHM

This section develops a low-complexity iterative algorithm based on the SPCA method [26], which has been extensively applied to efficiently solving the non-convex problems which arise in wireless communication systems design, e.g., [16], [22], [28]. Observe that (10) also has a non-concave objective function and constraint (9c) with the involved variables, and thus cannot be solved efficiently. Hence, we perform a few equivalent transformations to make the problem tractable, along with a few convex approximations to non-convex components.

A. EQUIVALENT TRANSFORMATIONS

We start by dealing with the non-concave objective (10a) and constraint (9c), and re-write (10) equivalently as

$$\min_{\mathbf{W},\mathbf{p},\mathbf{t}} \ \left\|\tilde{\mathbf{q}}_{\text{D}}\right\|_2 + \left\|\tilde{\mathbf{q}}_{\text{U}}\right\|_2 \tag{11a}$$

$$\text{s.t.} \ \gamma_{i,n}^{\text{D}} \geq e^{t_{i,n}^{\text{D}}} - 1, \quad \forall i \in \mathcal{D}, \ \forall n, \tag{11b}$$

$$\gamma_{j,n}^{\text{U}} \geq e^{t_{j,n}^{\text{U}}} - 1 \quad \forall j \in \mathcal{U}, \ \forall n, \tag{11c}$$

$$\sum_{n=1}^{N} \sum_{i \in \mathcal{D}_b} \text{tr}(\mathbf{W}_{i,n}) \leq P_{b,\max} \quad \forall b, \tag{11d}$$

$$P_b^{\text{cir}} + \sum_{n=1}^{N} \Big(\sum_{j \in \mathcal{U}_b} \alpha_j t_{j,n}^{\text{U}} + \sum_{i \in \mathcal{D}_b} \text{tr}(\mathbf{W}_{i,n}) \Big) \leq P_b \quad \forall b, \tag{11e}$$

$$(9\text{d}), \ (9\text{f}), \ (9\text{g}), \tag{11f}$$

where $\mathbf{t} = \{\mathbf{t}_1, \ldots, \mathbf{t}_{B+1}\}$, with $\mathbf{t}_b = [t_{\mathcal{D}_b(1),1}^{\text{D}}, \ldots, t_{\mathcal{D}_b(|\mathcal{D}_b|),N}^{\text{D}}, t_{\mathcal{U}_b(1),1}^{\text{U}} \ldots, t_{\mathcal{U}_b(|\mathcal{U}_b|),N}^{\text{U}}]$,[3] and $\mathbf{t}_b \geq 0 \, \forall b$ is a vector of newly introduced slack variables. Further, $\tilde{\mathbf{q}}_{\text{D}} = Q_i^{\text{D}} - \sum_{n=1}^{N} t_{i,n}^{\text{D}}$ and $\tilde{\mathbf{q}}_{\text{U}} = Q_j^{\text{U}} - \sum_{n=1}^{N} t_{j,n}^{\text{U}}$. The equivalence of (10) and (11) is due to the fact that constraints (11b) and (11c) are active at the optimum and that maximizing $\mathbf{t}$ maximizes the SINR (2), and consequently, minimizes the objective function. After the above transformation, the objective function becomes convex and the constraint (11e) becomes linear with respect to (w.r.t.) the involved variables. However, problem (11) is still non-convex because of the non-convex constraints (11b) and (11c). We tackle these non-convex constraints one by one by equivalently transforming them into tractable forms. First, by introducing a set of new variables $\boldsymbol{\beta} = \{\boldsymbol{\beta}_1, \ldots, \boldsymbol{\beta}_{B+1}\}$, with $\boldsymbol{\beta}_b = [\beta_{\mathcal{D}_b(1),1}, \ldots, \beta_{\mathcal{D}_b(|\mathcal{D}_b|),N}]$, the non-convex constraint (11b) can be expressed equivalently as

$$\mathbf{h}_{b_i,i,n}^H \mathbf{W}_{i,n} \mathbf{h}_{b_i,i,n} \geq (e^{t_{i,n}^{\text{D}}} - 1)\beta_{i,n}, \tag{12a}$$

$$\sigma_n^2 + \sum_{k \neq i}^{K_{\text{D}}} \mathbf{h}_{b_k,i,n}^H \mathbf{W}_{k,n} \mathbf{h}_{b_k,i,n} + \sum_{j=1}^{K_{\text{U}}} p_{j,n} |g_{j,i,n}|^2 \leq \beta_{i,n}, \tag{12b}$$

where (12b) is convex. The variable $\beta_{i,n}$ is essentially the maximum interference-plus-noise received by DL UE i on sub-channel n. Constraint (12a) can be made more tractable by decomposing it into the following inequalities:

$$\mathbf{h}_{b_i,i,n}^H \mathbf{W}_{i,n} \mathbf{h}_{b_i,i,n} \geq z_{i,n}^{\text{D}} \beta_{i,n}, \tag{13a}$$

$$e^{t_{i,n}^{\text{D}}} \leq z_{i,n}^{\text{D}} + 1, \tag{13b}$$

where $z_{i,n}^{\text{D}} \geq 0 \, \forall i \in \mathcal{D}, \forall n$ are the newly introduced variables. The equivalence of (12a) and (13) is attributed to the fact that inequalities (13a) and (13b) are active at the optimality. We now turn our attention to constraint (11c). We decompose the inequality in (11c) into a set of three new inequalities as

$$x_{j,n}^2 \mathbf{h}_{b_j,j,n}^H \mathbf{X}_{j,n}^{-1} \mathbf{h}_{b_j,j,n}, \geq z_{j,n}^{\text{U}}, \tag{14a}$$

$$p_{j,n} \geq x_{j,n}^2, \tag{14b}$$

$$e^{t_{j,n}^{\text{U}}} - 1 \leq z_{j,n}^{\text{U}}, \tag{14c}$$

where $\mathbf{X}_{j,n} \triangleq \sigma_n^2 \mathbf{I}_{M_R} + \sum_{l>j}^{K_{\text{U}}} p_{l,n} \mathbf{h}_{b_j,l,n} \mathbf{h}_{b_j,l,n}^H + \sum_{i=1}^{K_{\text{D}}} \mathbf{H}_{b_j,b_i,n}^H \mathbf{W}_{i,n} \mathbf{H}_{b_j,b_i,n}^H$, and $x_{j,n}^2$ and $z_{j,n}^{\text{U}} \geq 0 \, \forall j \in \mathcal{U}, \forall n$ are the auxiliary variables. The introduction of slack variable $x_{j,n}$ helps in identifying the convexity hidden in the right-hand side of (14a), which is useful in applying the convex approximation techniques in the next subsection. Constraints (14b) and (14c) are convex and only (14b) takes the SOC form.

Now, using the equivalent transformations discussed above, the relaxed problem (10) can be rewritten as

$$\min_{\mathbf{W},\mathbf{p},\boldsymbol{\beta},\mathbf{t},\mathbf{x},\mathbf{z}} \ \left\|\tilde{\mathbf{q}}_{\text{D}}\right\|_2 + \left\|\tilde{\mathbf{q}}_{\text{U}}\right\|_2 \tag{15a}$$

$$\text{s.t.} \quad \mathbf{h}_{b_i,i,n}^H \mathbf{W}_{i,n} \mathbf{h}_{b_i,i,n} \geq z_{i,n}^{\text{D}} \beta_{i,n} \quad \forall i \in \mathcal{D}, \ \forall n, \tag{15b}$$

$$e^{t_{i,n}^{\text{D}}} \leq z_{i,n}^{\text{D}} + 1 \quad \forall i \in \mathcal{D}, \ \forall n, \tag{15c}$$

$$\sigma_n^2 + \sum_{k \neq i}^{K_{\text{D}}} \mathbf{h}_{b_k,i,n}^H \mathbf{W}_{k,n} \mathbf{h}_{b_k,i,n} + \sum_{j=1}^{K_{\text{U}}} p_{j,n} |g_{j,i,n}|^2 \leq \beta_{i,n} \quad \forall i \in \mathcal{D}, \ \forall n, \tag{15d}$$

$$x_{j,n}^2 \mathbf{h}_{b_j,j,n}^H \mathbf{X}_{j,n}^{-1} \mathbf{h}_{b_j,j,n} \geq z_{j,n}^{\text{U}} \quad \forall j \in \mathcal{U}, n, \tag{15e}$$

$$p_{j,n} \geq x_{j,n}^2 \quad \forall j \in \mathcal{U}, \ \forall n, \tag{15f}$$

$$e^{t_{j,n}^{\text{U}}} \leq z_{j,n}^{\text{U}} + 1 \quad \forall j \in \mathcal{U}, \ \forall n, \tag{15g}$$

$$(9\text{d}), \ (9\text{f}), \ (9\text{g}), \ (11\text{d}), \ (11\text{e}). \tag{15h}$$

We observe that the transformed problem (15) is now more tractable as compared to the original form. However, it is still non-convex due to the presence of two non-convex constraints (15b) and (15e). To handle these two constraints,

[3] $\mathcal{B}(i)$ and $|\mathcal{B}|$ denote the ith element and cardinality of set $\mathcal{B}$, respectively.

in the next subsection, we approximate them with a convex function at a point of operation.

B. CONVEX APPROXIMATIONS

We start with (15b), where the right-hand side of the inequality is neither a convex nor a concave function of $z^{\mathrm{D}}_{i,n}$ and $\beta_{i,n}$. To overcome this obstacle, we first employ an upper bound convex approximation of the right-hand side by the following inequality as [26]

$$f(z^{\mathrm{D}}_{i,n}, \beta_{i,n}) = z^{\mathrm{D}}_{i,n}\beta_{i,n} \leq F(z^{\mathrm{D}}_{i,n}, \beta_{i,n}, \xi) \triangleq \frac{1}{2\xi}\beta^2_{i,n} + \frac{\xi}{2}(z^{\mathrm{D}}_{i,n})^2 \quad \forall \xi > 0. \tag{16}$$

For $\xi = \beta_{i,n}/z^{\mathrm{D}}_{i,n}$, we can easily check that

$$f(z_{i,n}, \beta_{i,n}) = F(z^{\mathrm{D}}_{i,n}, \beta_{i,n}, \xi), \tag{17}$$

$$\nabla f(z^{\mathrm{D}}_{i,n}, \beta_{\mathrm{D}i,b,n}) = \nabla F(z^{\mathrm{D}}_{i,n}, \beta_{i,n}, \xi), \tag{18}$$

where ∇f denotes the gradient of f. With the satisfaction of the above two conditions, the local convergence of the iterative algorithm can be established [29].

Next, we turn our attention to the non-convex inequality (15e), which can be expressed equivalently as $z^{\mathrm{U}}_{j,n} - x^2_{j,n}\mathbf{h}^H_{b_j,j,n}\mathbf{X}^{-1}_{j,n}\mathbf{h}_{b_j,j,n} \leq 0$. According to [16] and [30], $h(x_{j,n}, \mathbf{p}_{\mathcal{U}\setminus\{j\}}, \mathbf{W}) = x^2_{j,n}\mathbf{h}^H_{b_j,j,n}\mathbf{X}^{-1}_{j,n}\mathbf{h}_{b_j,j,n}$ is jointly convex w.r.t. the variables involved, where $\mathbf{p}_{\mathcal{U}\setminus\{j\}}$ is a vector, which consists of all UL UEs power coefficients except the jth UE. In order to make the non-convex inequality convex, we approximate $-h(x_{j,n}, \mathbf{p}_{\mathcal{U}\setminus\{j\}}, \mathbf{W})$ with a first-order approximation around a feasible point $(x_{j,n}(r), \mathbf{p}_{\mathcal{U}\setminus\{j\}}(r), \mathbf{W}(r))$ as follows

$$\begin{aligned} &h(x_{j,n}, \mathbf{p}_{\mathcal{U}\setminus\{j\}}, \mathbf{W}) \\ &\leq H(x_{j,n}, \mathbf{p}_{\mathcal{U}\setminus\{j\}}, \mathbf{W}, x_{j,n}(r), \mathbf{p}_{\mathcal{U}\setminus\{j\}}(r), \mathbf{W}(r)) \\ &= h(x_{j,n}(r), \mathbf{p}_{\mathcal{U}\setminus\{j\}}(r), \mathbf{W}(r)) - 2x_{j,n}(r)\mathbf{h}^H_{b_j,j,n}(\mathbf{X}_{j,n}(r))^{-1} \\ &\quad \times \mathbf{h}_{b_j,j,n}(x_{j,n} - x_{j,n}(r)) + \mathrm{tr}\big[(x_{j,n}(r))^2(\mathbf{X}_{j,n}(r))^{-1}\mathbf{h}_{b_j,j,n} \\ &\qquad \mathbf{h}^H_{b_j,j,n}(\mathbf{X}_{j,n}(r))^{-1}(\mathbf{X}_{j,n} - (\mathbf{X}_{j,n}(r))^{-1})\big], \end{aligned} \tag{19}$$

where r is the iteration index. Note that the above approximation satisfies the three conditions mentioned in [29], which are important to ensure the local convergence of the iterative algorithm.

By applying the approximations discussed above, and denoting $\mathbf{z} = \{\mathbf{z}_1, \ldots, \mathbf{z}_{B+1}\}$, where $\mathbf{z}_b = [z^{\mathrm{D}}_{\mathcal{D}_b(1),1}, \ldots, z^{\mathrm{D}}_{\mathcal{D}_b(|\mathcal{D}_b|),N}, z^{\mathrm{U}}_{\mathcal{U}_b(1),1} \ldots, z^{\mathrm{U}}_{\mathcal{U}_b(|\mathcal{U}_b|),N}]$ and $\mathbf{x} = \{\mathbf{x}_1, \ldots, \mathbf{x}_{B+1}\}$, where $\mathbf{x}_b = [x_{\mathcal{U}_b(1),1}, \ldots, x_{\mathcal{U}_b(|\mathcal{U}_b|),N}]$, problem (10) can be solved by iteratively solving the following approximated convex problem, which is formulated at the $(r+1)$th iteration index as

$$\min_{\mathcal{X}} \ \|\tilde{\mathbf{q}}_{\mathrm{D}}\|_2 + \|\tilde{\mathbf{q}}_{\mathrm{U}}\|_2 \tag{20a}$$

$$\text{s.t. } \mathbf{h}^H_{b_i,i,n}\mathbf{W}_{i,n}\mathbf{h}_{b_i,i,n} \geq F(z^{\mathrm{D}}_{i,n}, \beta_{i,n}, \xi(r)) \quad \forall i \in \mathcal{D}, \ \forall n, \tag{20b}$$

$$H(x_{j,n}, \mathbf{p}_{\mathcal{U}\setminus\{j\}}, \mathbf{W}, x_{j,n}(r), \mathbf{p}_{\mathcal{U}\setminus\{j\}}(r), \mathbf{W}(r)) \leq z^{\mathrm{U}}_{j,n} \quad \forall j \in \mathcal{U}, \ \forall n, \tag{20c}$$

$$\text{(9d), (9f), (9g), (11d), (11e), (15c), (15d), (15f), (15g).} \tag{20d}$$

where $\mathcal{X} = \{\mathcal{X}_1, \ldots, \mathcal{X}_{B+1}\}$ and $\mathcal{X}_b$ collects the variables corresponding to the BS b, i.e., $\{\mathbf{W}_b, \mathbf{p}_b, \boldsymbol{\beta}_b, \mathbf{t}_b, \mathbf{x}_b, \mathbf{z}_b\}$. Note that $\boldsymbol{\beta}$, $\mathbf{t}$, $\mathbf{x}$, and $\mathbf{z}$ are not the actual optimization variables; however, they get updated by the optimum values at the end of each iteration. By denoting $\mathbf{h} = [\mathbf{h}_{1,1,1}, \ldots, \mathbf{h}_{B,K_{\mathrm{D}},N}]$ and $\mathbf{g} = [g_{1,1,1}, \ldots, g_{K_{\mathrm{D}},K_{\mathrm{U}},N}]$, the pseudo code for the proposed resource allocation optimization algorithm for FD small cell (RAOFDS) is summarized in Algorithm 1. After the algorithm converges, a rank-one solution is obtained using the randomization trick [31].

Algorithm 1 Centralized Iterative Resource Allocation Optimization for Full-Duplex Small Cell (RAOFDS) Algorithm

Input: $\mathbf{h}$, $\mathbf{g}$, σ^2_n, P^{cir}_b, $P_{b,\max}$, P_b, α, $P_{u,\max}$ $I_{\max,1}$.
Output: $\mathbf{W}$, $\mathbf{p}$.

1: Initialize $\mathbf{W}(r)$, $\mathbf{p}(r)$, $\boldsymbol{\beta}(r)$, $\mathbf{t}(r)$, $\mathbf{x}(r)$, $\mathbf{z}(r)$
2: Set $r := 0$;
3: **repeat**
4: Solve (20) for local optimal values of $\mathbf{w}^\star$, $\mathbf{p}^\star$, $\boldsymbol{\beta}^\star$, $\mathbf{t}^\star$, $\mathbf{x}^\star$, $\mathbf{z}^\star$;
5: Set $r := r + 1$;
6: Update $\mathbf{w}(r) = \mathbf{w}^\star$, $\mathbf{p}(r) = \mathbf{p}^\star$, $\boldsymbol{\beta}(r) = \boldsymbol{\beta}^\star$, $\mathbf{t}(r) = \mathbf{t}^\star$, $\mathbf{x}(r) = \mathbf{x}^\star$, $\mathbf{z}(r) = \mathbf{z}^\star$, $\xi_{i,n}(r) = \beta^\star_{i,n}/z^\star_{i,n} \quad \forall i, \forall n$;
7: **until** Queue convergence or $r \geq I_{\max,1}$
8: Perform randomization to extract a rank-one solution.

C. EXPONENTIAL CONE APPROXIMATION

Furthermore, we observe that constraints (15c) and (15g) are exponential cone; hence, problem (20) is considered as a generalized nonlinear convex program, which can be solved by using nonlinear solvers, e.g., Matlab's `Fmincon`. In general, the nonlinear solver has a high complexity and thus, requires a large number of iterations to converge. Problem (20) can be solved with lower complexity by approximating the exponential cone constraints as second-order cone (SOC) constraints [32]. A generic inequality of type $e^x \leq y$ can be approximated by a system of conic inequalities as

$$\kappa_{m+4} \leq y, \tag{21a}$$

$$||2 + x/2^{m-1} \quad 1 - \kappa_1||_2 \leq 1 + \kappa_1, \tag{21b}$$

$$||5/3 + x/2^m \quad 1 - \kappa_2||_2 \leq 1 + \kappa_2, \tag{21c}$$

$$||2\kappa_1 \quad 1 - \kappa_3||_2 \leq 1 + \kappa_3, \tag{21d}$$

$$19/17 + \kappa_2 + 1/24\kappa_3 \leq \kappa_4, \tag{21e}$$

$$||2\kappa_{i-1} \quad 1 - \kappa_i||_2 \leq 1 + \kappa_i, \quad i = 5, 6, \ldots, m+3, \tag{21f}$$

$$||2\kappa_{m+3} \quad 1 - \kappa_{m+4}||_2 \leq 1 + \kappa_{m+4}, \tag{21g}$$

where the parameter m determines the accuracy of the approximation and $\kappa_i, i = 1, \ldots, (m+4)$ are newly introduced variables.

D. CONVERGENCE AND COMPLEXITY ANALYSIS

For the convergence analysis of Algorithm 1, we follow the steps outlined in [26]. First, we denote the return objective function value and a set of feasible optimal solutions at the rth iteration of the algorithm by $J(r)$ and $\Xi(r)$, respectively. Then, because of the convex approximation in (20b) and the linear approximation in (20c), the updating rule in Algorithm 1 ensures that $\Xi(r)$ is feasible at the $(r+1)$th iteration. Consequently, $J(r+1) \leq J(r)$ always holds and hence, Algorithm 1 yields a non-increasing sequence of objective function values. Furthermore, since the objective function J is bounded from below and above due to the $\|\cdot\|_2 \geq 0$ and total transmit power constraints, respectively, the convergence of Algorithm 1, w.r.t. the objective function values is guaranteed.

The worse case per-iteration computational cost of Algorithm 1 is discussed. Since (20) is a SOC program, we use the result from [33] to calculate the computational cost of solving the problem. In the complexity calculation, we replace each exponential cone constraint of (20) with the approximate SOC constraints, i.e., (21). After the replacements, the problem has $NB(m+8)(K_{\mathrm{D}}+K_{\mathrm{U}})$ variables, and K_{U} SOC constraints of size K_{U}, and $(K_{\mathrm{D}}+K_{\mathrm{U}})(m+4)$ constraints of size 3. Thus, the worse case per-iteration computational cost of solving the problem is $\mathcal{O}(NB(m+8)(K_{\mathrm{U}}^3+K_{\mathrm{U}}^2K_{\mathrm{D}}+(K_{\mathrm{U}}^2+K_{\mathrm{D}}^2)(m+4)))$, where the small order terms are ignored.

IV. DISTRIBUTED SOLUTION

Note that the algorithm developed in the previous section requires the global channel state information (CSI) knowledge to arrive at a solution and is referred to as the centralized algorithm. Acquiring the global CSI needs extra resources and it is practically impossible for a dense network. Thus, in this section, we apply a practical distributed approach to solve (20), where the MBS and SBSs only need to know local CSI. Moreover, turning to a distributed approach is evident as it avoids the exchange of overwhelming overhead data. In this approach, each BS independently designs the beamformers and power allocations of the local UEs with minimal exchange of a few control variables among the BSs.

In order to implement a distributed approach, we employ the dual decomposition framework [34] and follow similar steps as in [35]. In this technique, a large separable problem is decomposed into smaller sub-problems that can be solved efficiently. Owing to the separability of the objective function w.r.t. each BS, (20) can be written equivalently as

$$\underset{\mathcal{X}}{\text{minimize}} \quad \sum_{b\in\mathcal{B}} \left\|\tilde{\mathbf{q}}_{\mathrm{D},b}\right\|_2 + \sum_{b\in\mathcal{B}} \left\|\tilde{\mathbf{q}}_{\mathrm{U},b}\right\|_2 \tag{22a}$$

$$\text{s.t.} \quad (20\text{b}) - (20\text{d}), \tag{22b}$$

where $\tilde{\mathbf{q}}_{\mathrm{D},b}$ and $\tilde{\mathbf{q}}_{\mathrm{U},b}$ denote the queue deviations of the DL and UL UEs associated to b, respectively. However, constraints in (22b) are not separable; in particular, constraints (15d) and (20c) are coupled through the inter-cell CCI terms. To this end, we rewrite (22) as

$$\min_{\mathcal{X}} \sum_{b\in\mathcal{B}} \left\|\tilde{\mathbf{q}}_{\mathrm{D},b}\right\|_2 + \sum_{b\in\mathcal{B}} \left\|\tilde{\mathbf{q}}_{\mathrm{U},b}\right\|_2 \tag{23a}$$

$$\text{s.t.} \quad \sigma_n^2 + \sum_{k\in\mathcal{D}_b\setminus\{i\}} \mathbf{h}_{b_k,i,n}^H \mathbf{W}_{k,n} \mathbf{h}_{b_k,i,n} + \sum_{\bar{b}\in\bar{\mathcal{B}}_b} \psi_{\bar{b},i,n}^{(b)} + \sum_{j\in\mathcal{U}_b} p_{j,n}|g_{j,i,n}|^2 + \sum_{\bar{b}\in\bar{\mathcal{B}}_b} \phi_{\bar{b},i,n}^{(b)} \leq \beta_{i,n} \quad \forall i \in \mathcal{D},\ \forall n, \tag{23b}$$

$$\psi_{b,i,n}^{(b)} \geq \sum_{k\in\mathcal{D}_b} \mathbf{h}_{b,i,n}^H \mathbf{W}_{k,n} \mathbf{h}_{b,i,n} \quad \forall b,\ \forall i \in \bar{\mathcal{D}}_b,\ \forall n, \tag{23c}$$

$$\phi_{b,i,n}^{(b)} \geq \sum_{l\in\mathcal{U}_b} p_{l,n}|g_{l,i,n}|^2 \quad \forall b,\ \forall i \in \bar{\mathcal{D}}_b,\ \forall n, \tag{23d}$$

$$\mathbf{\Psi}_{b,j,n}^{(b)} \succeq \sum_{l\in\mathcal{U}_b} p_{l,n} \mathbf{h}_{b_j,l,n} \mathbf{h}_{b_j,l,n}^H \quad \forall b,\ \forall j \in \bar{\mathcal{U}}_b, \forall n, \tag{23e}$$

$$\mathbf{\Phi}_{b,j,n}^{(b)} \succeq \sum_{i\in\mathcal{D}_b} \mathbf{H}_{b,b_j,n} \mathbf{W}_{i,n} \mathbf{H}_{b,b_j,n}^H \quad \forall b,\ \forall j \in \bar{\mathcal{U}}_b,\ \forall n, \tag{23f}$$

$$\psi_{b,i,n}^{(b)} = \psi_{b,i,n}^{(b_i)} \quad \forall b \in \bar{\mathcal{B}}_{b_i},\ \forall i,\ \forall n, \tag{23g}$$

$$\phi_{b,i,n}^{(b)} = \phi_{b,i,n}^{(b_i)} \quad \forall b \in \bar{\mathcal{B}}_{b_i},\ \forall i,\ \forall n, \tag{23h}$$

$$\mathbf{\Psi}_{b,j,n}^{(b)} = \mathbf{\Psi}_{b,j,n}^{(b_j)} \quad \forall b \in \bar{\mathcal{B}}_{b_j},\ \forall j,\ \forall n, \tag{23i}$$

$$\mathbf{\Phi}_{b,j,n}^{(b)} = \mathbf{\Phi}_{b,j,n}^{(b_j)} \quad \forall b \in \bar{\mathcal{B}}_{b_j},\ \forall j,\ \forall n, \tag{23j}$$

$$(9\text{d}),\ (9\text{f}),\ (9\text{g}),\ (11\text{d}),\ (11\text{e}),\ (15\text{d}),\ (15\text{f}),\ (15\text{g}), \tag{23k}$$

where $\bar{\mathcal{B}}_b$, $\bar{\mathcal{D}}_b$ and $\bar{\mathcal{U}}_b$ denote the sets $\mathcal{B}\setminus\{b\}$, $\mathcal{D}\setminus\{\mathcal{D}_b\}$ and $\mathcal{U}\setminus\{\mathcal{U}_b\}$, respectively. Here, $\mathbf{X}_{j,n} \triangleq \sigma_n^2\mathbf{I}_{M_R} + \sum_{l>j}^{|\mathcal{U}_b|} p_{l,n}\mathbf{h}_{b_j,l,n}\mathbf{h}_{b_j,l,n}^H + \sum_{\bar{b}\neq b}^{B} \mathbf{\Psi}_{\bar{b},j,n}^{(b)} + \sum_{i=1}^{|\mathcal{D}_b|} \mathbf{H}_{b_j,b_i,n}^H \mathbf{W}_{i,n} \mathbf{H}_{b_j,b_i,n}^H + \sum_{\bar{b}\neq b}^{B} \mathbf{\Phi}_{\bar{b},j,n}^{(b)}$. $\psi_{b,i,n}$ and $\phi_{b,i,n}$ are newly introduced positive auxiliary variables, respectively, representing the inter-cell CCI caused by the DL and UL transmissions of BS b to the neighboring cells DL UE $i \in \bar{\mathcal{D}}_b$. Similarly, $\mathbf{\Psi}_{b,j,n}$ and $\mathbf{\Phi}_{b,j,n}$ are newly introduced PSD auxiliary matrix variables, respectively, representing the inter-cell CCI covariance matrices caused by the UL and DL transmissions of the BS b to the neighboring cells UL UE $j \in \bar{\mathcal{U}}_b$. The equality constraints (23g)-(23j) are introduced to further simplify the decoupling. They essentially say that the coupling interference variable must be equal, e.g., $\psi_{b,i,n}\,\forall i \in \bar{\mathcal{D}}_b$ couples exactly two BSs, i.e., the generating BS b and the interference receiving BS b_i [35]. Superscript $(\cdot)$ denotes the local copy of the variable. The equivalence between (22) and (23) is due to the fact that constraints (23b)-(23f) hold with equality at optimality. Furthermore, if we allow these variables to be fixed, (23) can easily be decoupled into $B+1$ independent subproblems w.r.t. each BS.

In order to decouple the above problem, we apply the dual decomposition technique. For that, we first write the partial

Lagrangian dual of (23) w.r.t. the equality constraints as

$$\begin{aligned}
&\mathcal{L}(\mathcal{X}, \boldsymbol{\psi}, \boldsymbol{\phi}, \boldsymbol{\Phi}, \boldsymbol{\theta}, \boldsymbol{\omega}, \boldsymbol{\Theta}, \boldsymbol{\Omega}) \\
&= \sum_{b\in\mathcal{B}} \left\|\tilde{\mathbf{q}}_{\mathrm{D},b}\right\|_2 + \sum_{b\in\mathcal{B}} \left\|\tilde{\mathbf{q}}_{\mathrm{U},b}\right\|_2 \\
&\quad + \sum_{n=1}^{N} \sum_{i\in\mathcal{D}_b} \sum_{b\in\bar{\mathcal{B}}_{b_i}} \theta_{b,i,n}(\psi_{b,i,n}^{(b)} - \psi_{b,i,n}^{(b_i)}) \\
&\quad + \sum_{n=1}^{N} \sum_{i\in\mathcal{D}_b} \sum_{b\in\bar{\mathcal{B}}_{b_i}} \omega_{b,i,n}(\phi_{b,i,n}^{(b)} - \phi_{b,i,n}^{(b_i)}) \\
&\quad + \sum_{n=1}^{N} \sum_{j\in\mathcal{U}_b} \sum_{b\in\bar{\mathcal{B}}_{b_j}} \mathrm{tr}(\boldsymbol{\Theta}_{b,j,n}(\boldsymbol{\Psi}_{b,j,n}^{(b)} - \boldsymbol{\Psi}_{b,j,n}^{(b_j)})) \\
&\quad + \sum_{n=1}^{N} \sum_{j\in\mathcal{U}_b} \sum_{b\in\bar{\mathcal{B}}_{b_j}} \mathrm{tr}(\boldsymbol{\Omega}_{b,j,n}(\boldsymbol{\Phi}_{b,j,n}^{(b)} - \boldsymbol{\Phi}_{b,j,n}^{(b_j)})) \qquad (24) \\
&= \sum_{b\in\mathcal{B}} \left\|\tilde{\mathbf{q}}_{\mathrm{D},b}\right\|_2 + \sum_{b\in\mathcal{B}} \left\|\tilde{\mathbf{q}}_{\mathrm{U},b}\right\|_2 \\
&\quad + \sum_{b\in\mathcal{B}} \sum_{n=1}^{N} \Big(\sum_{i\in\bar{\mathcal{D}}_b} \theta_{b,i,n}\psi_{b,i,n}^{(b)} - \sum_{\bar{b}\in\bar{\mathcal{B}}_b} \sum_{i\in\mathcal{D}_b} \theta_{\bar{b},i,n}\psi_{\bar{b},i,n}^{(b)} \Big) \\
&\quad + \sum_{b\in\mathcal{B}} \sum_{n=1}^{N} \Big(\sum_{i\in\bar{\mathcal{D}}_b} \omega_{b,i,n}\phi_{b,i,n}^{(b)} - \sum_{\bar{b}\in\bar{\mathcal{B}}_b} \sum_{i\in\mathcal{D}_b} \omega_{\bar{b},i,n}\phi_{\bar{b},i,n}^{(b)} \Big) \\
&\quad + \sum_{b\in\mathcal{B}} \sum_{n=1}^{N} \Big(\sum_{j\in\bar{\mathcal{U}}_b} \mathrm{tr}(\boldsymbol{\Theta}_{b,j,n}\boldsymbol{\Psi}_{b,j,n}^{(b)}) \\
&\qquad\qquad - \sum_{\bar{b}\in\bar{\mathcal{B}}_b} \sum_{j\in\mathcal{U}_b} \mathrm{tr}(\boldsymbol{\Theta}_{\bar{b},j,n}\boldsymbol{\Psi}_{\bar{b},j,n}^{(b)}) \Big) \\
&\quad + \sum_{b\in\mathcal{B}} \sum_{n=1}^{N} \Big(\sum_{j\in\bar{\mathcal{U}}_b} \mathrm{tr}(\boldsymbol{\Omega}_{b,j,n}\boldsymbol{\Phi}_{b,j,n}^{(b)}) \\
&\qquad\qquad - \sum_{\bar{b}\in\bar{\mathcal{B}}_b} \sum_{j\in\mathcal{U}_b} \mathrm{tr}(\boldsymbol{\Omega}_{\bar{b},j,n}\boldsymbol{\Phi}_{\bar{b},j,n}^{(b)}) \Big), \qquad (25)
\end{aligned}$$

where $\theta_{b,i,n} \geq 0$, $\omega_{b,i,n} \geq 0\ \forall i,\ \forall b \in \bar{B}_{b_i}, \forall n$, are the real valued Lagrange multipliers associated with constraints (23g), (23h), and $\boldsymbol{\Theta}_{b,j,n} \succeq 0$, $\boldsymbol{\Omega}_{b,j,n} \succeq 0\ \forall j, \forall b \in \bar{B}_{b_j}, \forall n$ are PSD Lagrange multipliers associated with constraints (23i), and (23j), respectively. $\boldsymbol{\psi}$ and $\boldsymbol{\theta}$ collect $\{\boldsymbol{\psi}^{(1)}, \ldots, \boldsymbol{\psi}^{(B+1)}\}$ and $\{\boldsymbol{\theta}_1, \ldots, \boldsymbol{\theta}_{B+1}\}$, respectively. Variables $\boldsymbol{\psi}^{(b)}$ and $\boldsymbol{\theta}_b$ denote the collection of interference terms and Lagrangian multipliers corresponding to BS b and are expressed as

$$\begin{aligned}
\boldsymbol{\psi}^{(b)} = [&\psi_{b,\bar{\mathcal{D}}_b(1),1}^{(b)}, \ldots, \psi_{b,\bar{\mathcal{D}}_b(|\bar{\mathcal{D}}_b|),N}^{(b)}, \psi_{\bar{\mathcal{B}}_b(1),\mathcal{D}_b(1),1}^{(b)}, \ldots, \\
&\psi_{\bar{\mathcal{B}}_b(1),\mathcal{D}_b(|\mathcal{D}_b|),N}^{(b)}, \psi_{\bar{\mathcal{B}}_b(|\bar{\mathcal{B}}_b|),\mathcal{D}_b(1),1}^{(b)}, \ldots, \\
&\psi_{\bar{\mathcal{B}}_b(|\bar{\mathcal{B}}_b|),\mathcal{D}_b(|\mathcal{D}_b|),N}^{(b)}],
\end{aligned}$$

and

$$\begin{aligned}
\boldsymbol{\theta}_b = [&\theta_{b,\bar{\mathcal{D}}_b(1),1}, \ldots, \theta_{b,\bar{\mathcal{D}}_b(|\bar{\mathcal{D}}_b|),N}, -\theta_{\bar{\mathcal{B}}_b(1),\mathcal{D}_b(1),1}, \ldots, \\
&-\theta_{\bar{\mathcal{B}}_b(1),\mathcal{D}_b(|\mathcal{D}_b|),N}, -\theta_{\bar{\mathcal{B}}_b(|\bar{\mathcal{B}}_b|),\mathcal{D}_b(1),1}, \ldots, \\
&-\theta_{\bar{\mathcal{B}}_b(|\bar{\mathcal{B}}_b|),\mathcal{D}_b(|\mathcal{D}_b|),N}],
\end{aligned}$$

respectively. Other sets of variables in (24), i.e., $\boldsymbol{\phi}$, $\boldsymbol{\Psi}$, $\boldsymbol{\Phi}$, $\boldsymbol{\omega}$, $\boldsymbol{\Theta}$, and $\boldsymbol{\Omega}$ are similarly represented.

The dual objective function of (23) is given as

$$g(\boldsymbol{\theta}, \boldsymbol{\omega}, \boldsymbol{\Theta}, \boldsymbol{\Omega}) = \min_{\substack{\mathcal{X},\boldsymbol{\psi},\boldsymbol{\phi},\\ \boldsymbol{\Psi},\boldsymbol{\Phi}}} \mathcal{L}(\mathcal{X}, \boldsymbol{\psi}, \boldsymbol{\phi}, \boldsymbol{\Psi}, \boldsymbol{\Phi}, \boldsymbol{\theta}, \boldsymbol{\omega}, \boldsymbol{\Theta}, \boldsymbol{\Omega}) \qquad (26a)$$

$$\text{s.t} \quad (23c) - (23g), (23k), \qquad (26b)$$

and the corresponding dual problem is given as

$$\max_{\boldsymbol{\theta},\boldsymbol{\omega},\boldsymbol{\Theta},\boldsymbol{\Omega}} g(\boldsymbol{\theta}, \boldsymbol{\omega}, \boldsymbol{\Theta}, \boldsymbol{\Omega}). \qquad (27)$$

Finally, for fixed Lagrangian dual variables, the independent bth sub-problem is expressed as

$$\begin{aligned}
\min\ &\left\|\tilde{\mathbf{q}}_{\mathrm{D},b}\right\|_2 + \left\|\tilde{\mathbf{q}}_{\mathrm{U},b}\right\|_2 + \sum_{n=1}^{N} \Big(\sum_{i\in\bar{\mathcal{D}}_b} \theta_{b,i,n}\psi_{b,i,n}^{(b)} \\
&- \sum_{\bar{b}\in\bar{\mathcal{B}}_b} \sum_{i\in\mathcal{D}_b} \theta_{\bar{b},i,n}\psi_{b,i,n}^{(b)} \Big) + \sum_{n=1}^{N} \Big(\sum_{i\in\bar{\mathcal{D}}_b} \omega_{b,i,n}\phi_{b,i,n}^{(b)} \\
&- \sum_{\bar{b}\in\bar{\mathcal{B}}_b} \sum_{i\in\mathcal{D}_b} \omega_{\bar{b},i,n}\phi_{b,i,n}^{(b)} \Big) + \sum_{n=1}^{N} \Big(\sum_{j\in\bar{\mathcal{U}}_b} \mathrm{tr}(\boldsymbol{\Theta}_{b,j,n}\boldsymbol{\Psi}_{b,j,n}^{(b)}) \\
&\qquad - \sum_{\bar{b}\in\bar{\mathcal{B}}_b} \sum_{j\in\mathcal{U}_b} \mathrm{tr}(\boldsymbol{\Theta}_{\bar{b},j,n}\boldsymbol{\Psi}_{\bar{\mathcal{B}}_b(b),j,n}^{(b)}) \Big) \\
&+ \sum_{n=1}^{N} \Big(\sum_{j\in\bar{\mathcal{U}}_b} \mathrm{tr}(\boldsymbol{\Omega}_{b,j,n}\boldsymbol{\Phi}_{b,j,n}^{(b)}) \\
&\qquad - \sum_{\bar{b}\in\bar{\mathcal{B}}_b} \sum_{j\in\mathcal{U}_b} \mathrm{tr}(\boldsymbol{\Omega}_{\bar{b},j,n}\boldsymbol{\Phi}_{\bar{\mathcal{B}}_b(b),j,n}^{(b)}) \Big) \qquad (28a) \\
\text{s.t.}\ &\sigma_n^2 + \sum_{k\in\mathcal{D}_b\setminus\{i\}} \mathbf{h}_{b_k,i,n}^H \mathbf{W}_{k,n}\mathbf{h}_{b_k,i,n} \qquad (28b) \\
&+ \sum_{\bar{b}\in\bar{\mathcal{B}}_b} \psi_{\bar{b},i,n} + \sum_{j\in\mathcal{U}_b} p_{j,n}|g_{j,i,n}|^2 \\
&+ \sum_{\bar{b}\in\bar{\mathcal{B}}_b} \phi_{\bar{b},i,n} \leq \beta_{i,n} \quad \forall i \in \mathcal{D}_b,\ \forall n, \qquad (28c) \\
&\psi_{b,i,n}^{(b)} \geq \sum_{k\in\mathcal{D}_b} \mathbf{h}_{b,\bar{i},n}^H \mathbf{W}_{k,n}\mathbf{h}_{b,\bar{i},n} \quad \forall i \in \bar{\mathcal{D}}_b,\ \forall n, \qquad (28d) \\
&\phi_{b,i,n}^{(b)} \geq \sum_{l\in\mathcal{U}_b} p_{l,n}|g_{l,\bar{i},n}|^2 \quad \forall i \in \bar{\mathcal{D}}_b,\ n, \qquad (28e) \\
&\Psi_{b,j,n}^{(b)} \succeq \sum_{j\in\mathcal{U}_b} p_{j,n}\mathbf{h}_{b,\bar{j},n}\mathbf{h}_{b,\bar{j},n}^H \quad \forall j \in \bar{\mathcal{U}}_b,\ \forall n, \qquad (28f) \\
&\Phi_{b,j,n}^{(b)} \succeq \sum_{i\in\mathcal{D}_b} \mathbf{H}_{b,b_{\bar{j}},n}\mathbf{W}_{i,n}\mathbf{H}_{b,b_{\bar{j}},n}^H\ \forall j \in \bar{\mathcal{U}}_b,\ \forall n, \qquad (28g) \\
&(23k), \qquad (28h)
\end{aligned}$$

where the optimization variables are $\mathcal{X}_b$, $\boldsymbol{\psi}^{(b)}$, $\boldsymbol{\phi}^{(b)}$, $\boldsymbol{\Psi}^{(b)}$ and $\boldsymbol{\Phi}^{(b)}$. Upon solving (28) for $\boldsymbol{\psi}^{(b)}$, $\boldsymbol{\phi}^{(b)}$, $\boldsymbol{\Psi}^{(b)}$ and $\boldsymbol{\Phi}^{(b)}\ \forall b$ in the νth iteration, the interference terms are exchanged between BSs b and b_i as

$$\psi_{b,i,n}^{(b_i)}(\nu+1) = 0.5(\psi_{b,i,n}^{(b)} + \psi_{b,i,n}^{(b_i)}(\nu)) \quad \forall b, \forall i \in \bar{\mathcal{D}}_b, \forall n, \qquad (29)$$

$$\phi^{(b_i)}_{b,i,n}(v+1) = 0.5(\phi^{(b)}_{b,i,n} + \phi^{(b_i)}_{b,i,n}(v)) \quad \forall b, \forall i \in \bar{\mathcal{D}}_b, \forall n, \tag{30}$$

$$\boldsymbol{\Psi}^{(b_i)}_{b,i,n}(v+1) = 0.5(\boldsymbol{\Psi}^{(b)}_{b,i,n} + \boldsymbol{\Psi}^{(b_i)}_{b,i,n}(v)) \quad \forall b, \forall j \in \bar{\mathcal{U}}_b, \forall n, \tag{31}$$

$$\boldsymbol{\Phi}^{(b_i)}_{b,i,n}(v+1) = 0.5(\boldsymbol{\Phi}^{(b)}_{b,i,n} + \boldsymbol{\Phi}^{(b_i)}_{b,i,n}(v)) \quad \forall b, \forall j \in \bar{\mathcal{U}}_b, \forall n. \tag{32}$$

The solutions to the subproblems are optimal because of the convexity of (28). However, the obtained optimal solution may not be the optimal for (20) because the fixed dual variables are not optimal. Hence, we solve the master dual problem to obtain the optimal dual variables for the vth iteration using the subgradient method [30] as:

$$\theta_{b,i,n}(v+1) = [\theta_{b,i,n}(v) + \epsilon_1(v)(\psi^{(b)}_{b,i,n}(v) - \psi^{(b_i)}_{b,i,n}(v))] \quad \forall b, \forall i, \forall n, \tag{33}$$

$$\omega_{b,i,n}(v+1) = [\omega_{b,i,n}(v) + \epsilon_2(v)(\phi^{(b)}_{b,i,n}(v) - \phi^{(b_i)}_{b,i,n}(v))] \quad \forall b, \forall i, \forall n, \tag{34}$$

$$\boldsymbol{\Theta}_{b,j,n}(v+1) = [\boldsymbol{\Theta}_{b,j,n}(v) + \epsilon_3(v)(\boldsymbol{\Phi}^{(b)}_{b,j,n}(v) - \boldsymbol{\Phi}^{(b_j)}_{b,j,n}(v))^T] \quad \forall b, \forall j, \forall n, \tag{35}$$

$$\boldsymbol{\Omega}_{b,j,n}(v+1) = [\boldsymbol{\Omega}_{b,j,n}(v) + \epsilon_4(v)(\boldsymbol{\Psi}^{(b)}_{b,j,n}(v) - \boldsymbol{\Psi}^{(b_j)}_{b,j,n}(v))^T] \quad \forall b, \forall j, \forall n, \tag{36}$$

where ϵ_1, ϵ_2, ϵ_3, and ϵ_4 are the positive step sizes corresponding to the Lagrangian multipliers. The convergence properties of the dual problem is dependent on the proper selection of the step sizes. The pseudo code of the distributed algorithm is summarized in Algorithm 2.

Algorithm 2 Distributed Iterative resource allocation optimization for full-duplex small cell (RAOFDS) Algorithm

Input: $\mathbf{h}$, $\mathbf{g}$, σ_n, P^{cir}_b, $P_{b,\max}$, P_b, $P_{u,\max}$, α, $I_{\max,1}$, $I_{\max,2}$.
Output: $\mathbf{W}$, $\mathbf{p}$.

1: Initialize $\mathcal{X}(r)$ and initialize $\boldsymbol{\psi}(v)$, $\boldsymbol{\phi}(v)$, $\boldsymbol{\Psi}(v)$, $\boldsymbol{\Phi}(v)$, $\boldsymbol{\theta}(v)$, $\boldsymbol{\omega}(v)$, $\boldsymbol{\Theta}(v)$, $\boldsymbol{\Omega}(v)$ with all zero values.
2: Set $r := 0$; $v := 0$;
3: **repeat** BS $b \in \mathcal{B}$
4: **repeat**
5: Solve (28) for $\boldsymbol{\phi}^b(v)$, $\boldsymbol{\psi}^b(v)$, $\boldsymbol{\Psi}^b(v)$, and $\boldsymbol{\Phi}^b(v)$ and exchange them between the BSs;
6: Update Lagrange multipliers using (33)–(36);
7: Set $v := v + 1$;
8: **until** Convergence of Lagrange multipliers or $v \geq I_{\max,2}$
9: Update $\mathcal{X}(r) = \mathcal{X}^\star$ and $\xi_{i,n}(r) = \beta^\star_{i,n}/z^\star_{i,n} \quad \forall i \in \mathcal{D}_b, b \in \mathcal{B}, \forall n$;
10: $r := r + 1$; $v := 0$;
11: **until** Queue convergence or $r \geq I_{\max,1}$
12: Perform randomization to extract a rank-one solution.

V. NUMERICAL RESULTS AND DISCUSSIONS

In this section, we present the throughput performance results, which are obtained by using the centralized and distributed RAOFDS Algorithms 1 and 2, respectively, under various settings using Monte Carlo simulations.

We consider an urban outdoor deployment scenario with an MBS, which has the operating range of radius 500 m and is located at the origin in the plane $\mathbb{R}^2$. The SBSs, with the operating range of 50 m, are randomly deployed within the operating range of the MBS. The locations of SBSs follow an independent Poisson point process (PPP) $\Phi_s \in \mathbb{R}^2$ with intensity λ_s. The UEs are randomly positioned within the MBS operating range and their locations follow the PPP $\Phi_u \in \mathbb{R}^2$ with intensity λ_u. Every SBS and UE has the same maximum transmission power of $P_{b,\max}$ and $P_{u,\max}$, respectively. The SI channel between the co-located transmitter-receiver antenna pair of an SBS is modelled by using the Rician distribution as $\mathcal{CN}(\sqrt{\sigma^2_{\text{SI}}K/(1+K)}\mathbf{H}_{\text{SI}}, (\sigma^2_{\text{SI}}/(1+K))\mathbf{I}_{M_R} \otimes \mathbf{I}_{M_T})$, where $\mathbf{H}_{\text{SI}}$ is a deterministic matrix, K is the Rician factor with value 1, and σ^2_{SI} is the SI level represents the ratio of the average SI power before and after the SI cancellation stage. $\otimes$ is a Kronecker product operator. The other channels in the system are assumed to be Rayleigh faded. The path loss and shadowing loss between the various channels are calculated using the parameters mentioned in Table 1. All other system parameters used in simulations are summarized in Table 1. Furthermore, we consider three system scenarios for comparison, which are referred to as; i) Setup-A: SBSs are powered by the grid source, ii) Setup-B: SBSs are powered by a renewable energy source, and iii) Setup-C: SBSs are powered by a renewable energy source and draw energy for decoding UL UEs data. The Setup-A and B account for the energy consumed at the transmitter side operations and ignore the receiver side while the Setup-C accounts for both the sides operations simultaneously.

TABLE 1. Simulation parameters.

Parameters	Value
No. of antennas	$M_T = 2$, $M_R = 2$
No. of sub-carriers	$N = 2$
Cell radius	MBS: 500 m, SBS: 50 m
Maximum transmit power	SBS: 24 dBm, UE: 23 dBm
DE parameter	$\alpha = 0.1$
Circuit power	30 dBm
Bandwidth	10 MHz
Intensity	SBS: $\lambda_s = 10/\text{km}^2$, UE: $\lambda_u = 2\lambda_s$,
Thermal noise density and SI	-174 dBm/Hz, $\sigma^2_{\text{SI}} = -110$ dB
Noise figure	SBS: 13 dB, UE: 9 dB
Path loss (in dB) SBS-to-SBS where d is in km	LOS: $98.4 + 20.9\log_{10}(d)$ NLOS: $169.36 + 40\log_{10}(d)$
Path loss (in dB) UE-to-SBS where d is in km	LOS: $103.8 + 20.9\log_{10}(d)$ NLOS: $145.4 + 37.5\log_{10}(d)$
Path loss (in dB) UE-to-UE where d is in km	LOS: $98.5 + 20\log_{10}(d)$ NLOS: $175.78 + 40\log_{10}(d)$

Fig. 2 shows the typical placement of a MBS along with ten SBSs and their DL and UL UEs; these numbers are used in simulations, unless otherwise mentioned. The locations of the SBS and UEs are obtained using the values $\lambda_s = 10\,\text{km}^{-2}$ and $\lambda_u = 20\,\text{km}^{-2}$, respectively. Hence, we have a total of 10 SBSs, 20 DL and 20 UL UEs in the network. The UEs are assumed to be already associated either to a SBS or the MBS.

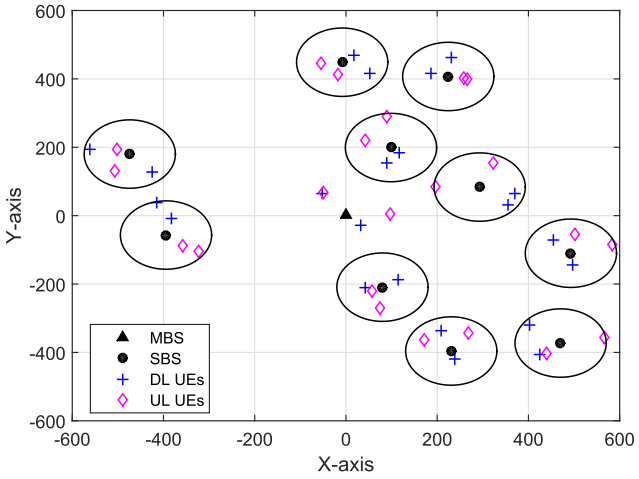

FIGURE 2. Location of MBS, SBSs, DL and UL UEs used in the simulations.

Particularly, in the simulation setup, two DL and two UL UEs are associated to each SBS. The UEs which are out of range of any SBS get associated to the MBS. The number of bits waiting in the data buffer of each DL and UL UE are stored in vectors as $Q^{\mathrm{D}} = [6745322223112223223700]$ and $Q^{\mathrm{U}} = [3735732313333122223211]$, respectively. The two zeros at the end in the Q^{D} vector are inserted to ensure that no DL transmission at the MBS. The energy harvesting rate at each SBS is assumed to be different from each other. Further, in numerical examples, the plots corresponding to the HD communications are obtained when the SBSs are operating in the frequency division duplexing mode and under the system setup-C. In particular, the DL UEs share one half and UL UEs share another half of the total system bandwidth for their respective transmissions.

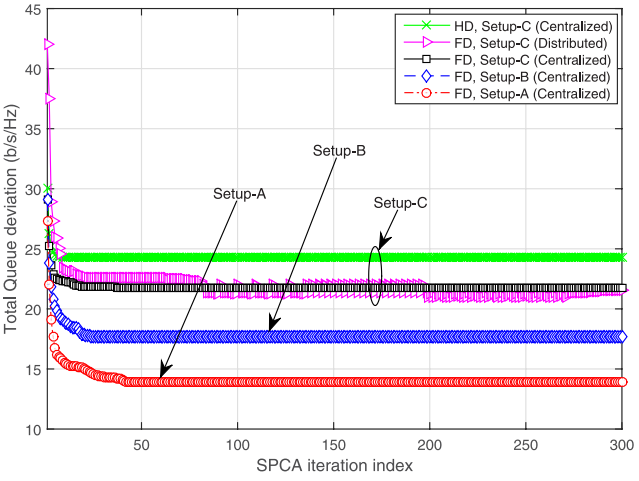

FIGURE 3. Convergence of the proposed SPCA-based RAOFDS algorithm with respect to the SPCA iteration index.

We first discuss the convergence behavior of the proposed centralized and distributed RAOFDS algorithms. In Fig. 3, the total number of bits that remain in the network is plotted after each SPCA iteration step. Firstly, it can be verified that the FD communications achieve higher total queue deviation than the conventional HD communications. Secondly, it can be verified that the centralized algorithm, which is plotted for system setups A, B and C, converges after approximately 65 iterations. Furthermore, from the figure we can also observe the significant performances gaps among the setup A, B and C. Specifically, Setup-C has a higher number of bits left in the network when compared with Setup-A and Setup-B. It is worth mentioning that the system settings used in Setup-C are the closest to a real situation, and offer optimal usage of resources available in a network under that situation. On the other hand, the distributed algorithm, which is plotted for system Setup-C, in Fig. 3, converges approximately after 290 iterations. The reason for this slow convergence lies in the dual decomposition method in which the objective function values start oscillating before arriving at the convergence.

For the sake of presentation clarity, we show the performance of the centralized Algorithm 1 in the rest of the section. It is worth noting that the distributed Algorithm 2 provides similar results when converges.

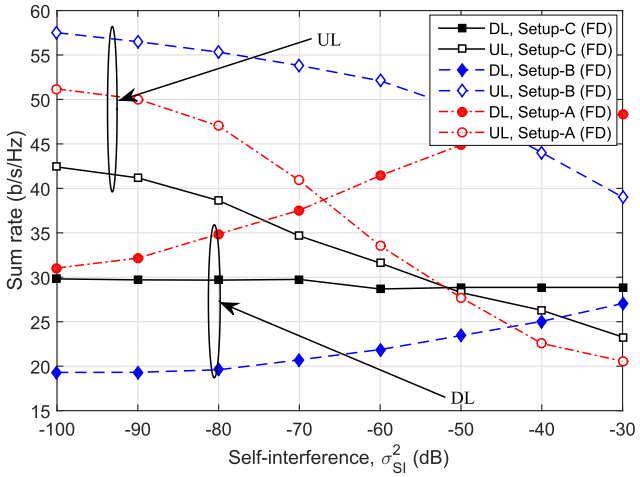

FIGURE 4. DL and UL sum rate of the network with different SI values used at each SBS.

In Fig. 4, the sum rate achieved by the DL and UL UEs with respect to the different values of SI variance is compared under three scenarios. As expected, the UL UEs sum rate decreases with the SI variance. That is, the better the isolation between the transmitter and receiver antennas of the SBS the higher the sum rate achieved by the UL UEs.

In Fig. 5, we study the effect of different normalized energy arrival rates, i.e., $P_{b,H}/(P_b^{\mathrm{cir}} + P_{b,\max})$, at the SBSs on the sum rate achieved by the DL and UL UEs for Setup-B and Setup-C. For simplicity, in this example, we assume that all SBSs have the same EH arrival rate. The sum rate achieved under Setup-A is independent of the energy arrivals; however, it is shown in the figure for comparison purposes. For Setup-B, when the energy arrival rate is low, the UL rate is higher than the DL rate as the SBS has lower available power for the DL UEs; thus, it causes less interference to the UL transmissions. In the high EH rate regime, the DL channels

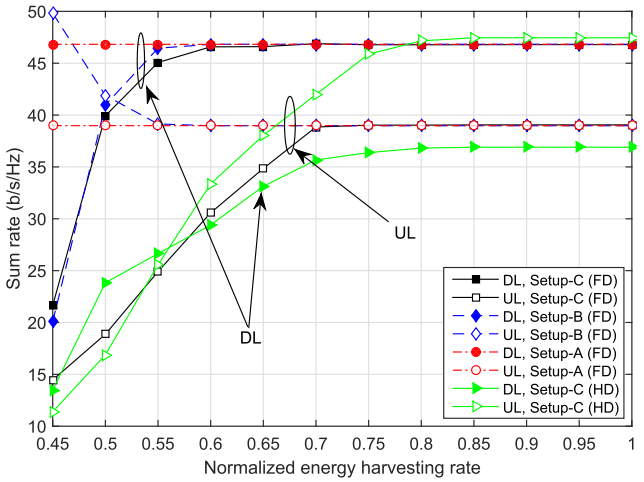

FIGURE 5. DL and UL sum rate of the network with different normalized EH arrival rates at each SBS.

achieve higher rate than the UL channels, which now receive higher interference from the high power DL transmissions. The situation is reversed for Setup-C, where the DL sum rates dominate in all EH rate regimes over the UL sum rates. In Setup-C, the SBS has to share the harvested energy between the DL and UL UEs. Lower energy availability at the SBS restricts the UL UEs to transmit at lower power, thus incurring less interference to the DL UEs. For the HD communications, we can observe that the total sum rate, which is an aggregate of the sum rate of DL and UL channels, improves with energy harvesting rate; however, remains lower than that of the FD communications.

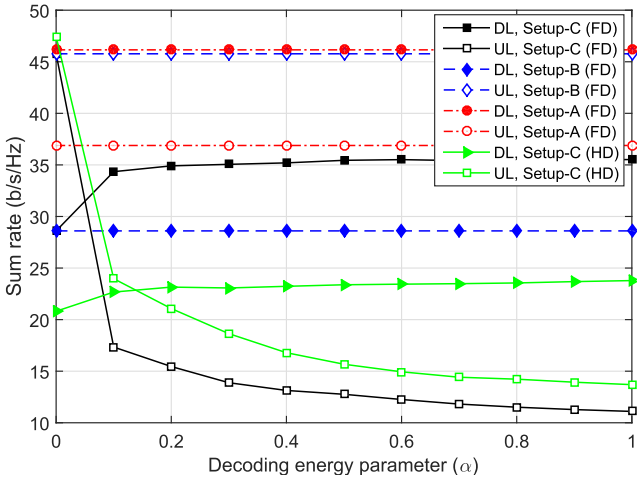

FIGURE 6. DL and UL sum rate versus the DE parameters used by each SBS.

In Fig. 6, we study the effect of the DE parameter on the achieved sum rates obtained for Setup-C. Although the sum rates of Setup-A and B are not affected by the DE parameter, they are plotted for comparison purposes. The UL sum rate decreases with the increase in the portion of DE consumed at the SBS. In Setup-C, the UL UEs rates are controlled by the availability of the DE at the SBS. If the values of the DE parameter is small, the SBS needs to share small portion of the available energy with the UL UEs in order to satisfy the power consumption constraint. This, in-effect, restricts the UL UEs from transmitting at lower power. Consequently, lower interference is experienced by the DL UEs, and thus, the sum rate has been improved as compared to Setup-B. High DE parameter values further restrict the UL UEs from transmitting at lower power, and hence DL UEs experience low interference. For the HD communications, which have no SI, the lower values of DE parameter allows the UL UEs to transmit at higher power while restricts them to use lower transmit power for the higher values of DE parameter. Hence, the UL and DL sum rate decreases and increases, respectively with the DE parameter values.

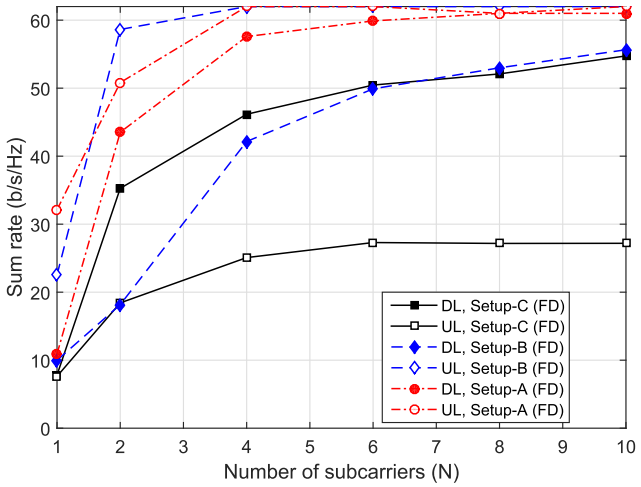

FIGURE 7. DL and UL sum rate of the network versus number of sub-carriers used in the network.

In Fig. 7, we compare the achieved sum rates for different numbers of sub-carriers employed by the network, under the three considered scenarios. In all cases, the sum rates increase with the number of sub-carriers, and worsen when the number of sub-carriers is limited to one. In such case, the interference seen by the UEs is the highest. The performance of the network improves significantly when the number of sub-carriers is two, as some interference among the DL and UL channels is avoided. The performance starts improving when more sub-carriers are employed by the network. When the number of sub-carriers is equal to the number of SBSs, each SBS communicates orthogonally on one sub-carrier, thus completely eliminating the inter-cell interference.

Finally, in Fig. 8, we compare the queue deviation of the network with different SBS deployment intensities, for the three considered scenarios. In this example, we assume that each UE has six bits of data in the queue at the beginning of the transmission period. The queue deviation of the network increases with the number of SBSs in all three setups. This is because using more SBSs generates an increased interference, which leads to a higher queue deviation. Furthermore, as expected, Setup-C sees a larger queue deviation due to the EH and DE consumption constraints.

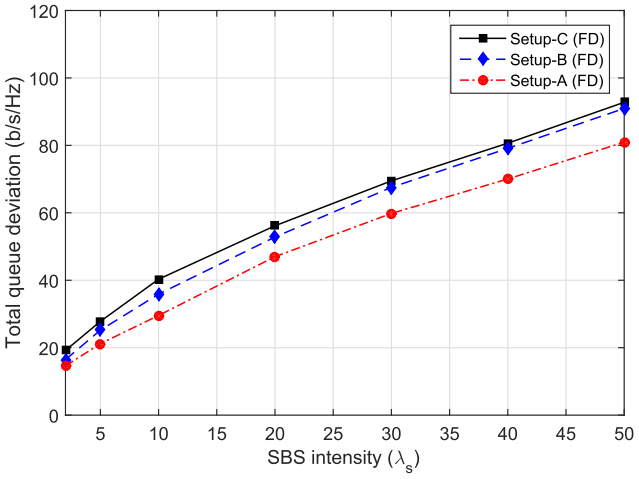

FIGURE 8. Total queue deviation of the network with SBS intensity.

VI. CONCLUSION

We have investigated the performance of densely deployed FD small cell BSs at the network level. We assume that each SBS for its transceiver operations depends on the energy collected from a renewable source. Owing to the SBS short range of operation, the energy required for performing the decoding of the UL UEs data is non-negligible and is a function of UEs data rates. Hence, the energy harvested at the SBS is shared among the DL and UL UEs. Under the practical energy consumption model, a joint beamformer and power allocation design, which minimizes the UEs data queue lengths, is proposed. The proposed optimization problem implicitly performs the sub-carrier allocation and UEs scheduling. A sub-optimal and iterative SPCA-based method is employed to circumvent the high-complexity approach in solving the non-convex problem. Centralized and decentralized algorithms are developed to solve the optimization problem. These algorithms have similar performances; however, the decentralized one requires less overheads while it exhibits a slower convergence. Through numerical simulations, the performances of the proposed design under the practical energy consumption model is compared with the case when the DE is ignored. Results show the performance gap and advocate the need for redesigning the beamformers and power allocations schemes. Results also validate that the FD communications achieve higher total queue deviation when compared to the HD communications.

REFERENCES

[1] N. Bhushan *et al.*, "Network densification: The dominant theme for wireless evolution into 5G," *IEEE Commun. Mag.*, vol. 52, no. 2, pp. 82–89, Feb. 2014.

[2] X. Huang, T. Han, and N. Ansari, "On green-energy-powered cognitive radio networks," *IEEE Commun. Surveys Tuts.*, vol. 17, no. 2, pp. 827–842, 2nd Quart., 2015.

[3] T. Han and N. Ansari, "Powering mobile networks with green energy," *IEEE Wireless Commun.*, vol. 21, no. 1, pp. 90–96, Feb. 2014.

[4] N. Ansari and T. Han, *Green Mobile Networks: A Networking Perspective*. Hoboken, NJ, USA: Wiley, 2017.

[5] O. Ozel, K. Tutuncuoglu, J. Yang, S. Ulukus, and A. Yener, "Transmission with energy harvesting nodes in fading wireless channels: Optimal policies," *IEEE J. Sel. Areas Commun.*, vol. 29, no. 8, pp. 1732–1743, Sep. 2011.

[6] T. Han and N. Ansari, "On optimizing green energy utilization for cellular networks with hybrid energy supplies," *IEEE Trans. Wireless Commun.*, vol. 12, no. 8, pp. 3872–3882, Aug. 2013.

[7] Z. Wang, V. Aggarwal, and X. Wang, "Iterative dynamic water-filling for fading multiple-access channels with energy harvesting," *IEEE J. Sel. Areas Commun.*, vol. 33, no. 3, pp. 382–395, Mar. 2015.

[8] D. W. K. Ng, E. S. Lo, and R. Schober, "Energy-efficient resource allocation in OFDMA systems with hybrid energy harvesting base station," *IEEE Trans. Wireless Commun.*, vol. 12, no. 7, pp. 3412–3427, Jul. 2013.

[9] I. Ahmed, A. Ikhlef, D. W. K. Ng, and R. Schober, "Power allocation for an energy harvesting transmitter with hybrid energy sources," *IEEE Trans. Wireless Commun.*, vol. 12, no. 12, pp. 6255–6267, Dec. 2013.

[10] A. Arafa and S. Ulukus, "Optimal policies for wireless networks with energy harvesting transmitters and receivers: Effects of decoding costs," *IEEE J. Sel. Areas Commun.*, vol. 33, no. 12, pp. 2611–2625, Dec. 2015.

[11] A. Yadav, T. M. Nguyen, and W. Ajib, "Optimal energy management in hybrid energy small cell access points," *IEEE Trans. Commun.*, vol. 64, no. 12, pp. 5334–5348, Dec. 2016.

[12] A. Goldsmith, *Wireless Communications*. New York, NY, USA: Cambridge Univ. Press, 2005.

[13] S. Hong *et al.*, "Applications of self-interference cancellation in 5G and beyond," *IEEE Commun. Mag.*, vol. 52, no. 2, pp. 114–121, Feb. 2014.

[14] D. Bharadia, E. McMilin, and S. Katti, "Full duplex radios," *SIGCOMM Comput. Commun. Rev.*, vol. 43, no. 4, pp. 375–386, Aug. 2013.

[15] M. Duarte and A. Sabharwal, "Full-duplex wireless communications using off-the-shelf radios: Feasibility and first results," in *Proc. Annu. Asilomar Conf. Signals, Syst., Comp.*, Pacific Grove, CA, USA, Nov. 2010, pp. 1558–1562.

[16] D. Nguyen, L.-N. Tran, P. Pirinen, and M. Latva-Aho, "On the spectral efficiency of full-duplex small cell wireless systems," *IEEE Trans. Wireless Commun.*, vol. 13, no. 9, pp. 4896–4910, Sep. 2014.

[17] S. Goyal, P. Liu, and S. S. Panwar, "User selection and power allocation in full-duplex multicell networks," *IEEE Trans. Veh. Technol.*, vol. 66, no. 3, pp. 2408–2422, Mar. 2016.

[18] Y. Li, P. Fan, L. Anatolii, and L. Liu, "On the spectral and energy efficiency of full-duplex small-cell wireless systems with massive MIMO," *IEEE Trans. Veh. Technol.*, vol. 66, no. 3, pp. 2339–2353, Mar. 2016.

[19] P. Grover, K. Woyach, and A. Sahai, "Towards a communication-theoretic understanding of system-level power consumption," *IEEE J. Select. Areas Commun.*, vol. 29, no. 8, pp. 1744–1755, Sep. 2011.

[20] S. Cui, A. J. Goldsmith, and A. Bahai, "Energy-efficiency of MIMO and cooperative MIMO techniques in sensor networks," *IEEE J. Sel. Areas Commun.*, vol. 22, no. 6, pp. 1089–1098, Aug. 2004.

[21] J. Rubio and A. Pascual-Iserte, "Energy-aware broadcast multiuser-MIMO precoder design with imperfect channel and battery knowledge," *IEEE Trans. Wireless Commun.*, vol. 13, no. 6, pp. 3137–3152, Jun. 2014.

[22] T. M. Nguyen, A. Yadav, W. Ajib, and C. Assi, "Energy efficiency with adaptive decoding power and wireless backhaul small cell selection," in *Proc. IEEE Global Telecommun. Conf.*, Washington, DC, USA, Dec. 2016, pp. 1–5.

[23] R. K. Mungara and A. Lozano, "Interference surge in full-duplex wireless systems," in *Proc. Annu. Asilomar Conf. Signals, Syst., Comp.*, Pacific Grove, CA, USA, Nov. 2015, pp. 25–29.

[24] A. C. Cirik, O. Taghizadeh, L. Lampe, R. Mathar, and Y. Hua, "Linear transceiver design for full-duplex multi-cell MIMO systems," *IEEE Access*, vol. 4, pp. 4678–4689, Aug. 2016.

[25] L. Chen, F. R. Yu, H. Ji, B. Rong, X. Li, and V. C. M. Leung, "Green full-duplex self-backhaul and energy harvesting small cell networks with massive MIMO," *IEEE J. Sel. Areas Commun.*, vol. 34, no. 12, pp. 3709–3724, Dec. 2016.

[26] A. Beck, A. Ben-Tal, and L. Tetruashvili, "A sequential parametric convex approximation method with applications to nonconvex truss topology design problems," *J. Global Optim.*, vol. 47, no. 1, pp. 29–51, May 2010.

[27] S. Cui, A. J. Goldsmith, and A. Bahai, "Power estimation for Viterbi decoders," Wireless Syst. Lab, Stanford Univ., Stanford, CA, USA, Tech. Rep. WSL-Shuguang-01, 2003.

[28] G. Venkatraman and A. Tölli, M. Juntti, and L. N. Tran, "Traffic aware resource allocation schemes for multi-cell MIMO-OFDM systems," *IEEE Trans. Signal Process.*, vol. 64, no. 11, pp. 2730–2745, Jun. 2016.

[29] B. R. Marks and G. P. Wright, "A general inner approximation algorithm for nonconvex mathematical programs," *Oper. Res.*, vol. 26, no. 4, pp. 681–683, 1978.
[30] S. Boyd and L. Vandenberghe, *Convex Optimization*, 1st ed. Cambridge, U.K.: Cambridge Univ. Press, 2004.
[31] N. D. Sidiropoulos, T. N. Davidson, and Z.-Q. Luo, "Transmit beamforming for physical-layer multicasting," *IEEE Trans. Signal Process.*, vol. 54, no. 6, pp. 2239–2251, Jun. 2006.
[32] A. Ben-Tal and A. Nemirovski, "On polyhedral approximations of the second-order cone," *Math. Operat. Res.*, vol. 26, no. 2, pp. 193–205, May 2001.
[33] M. S. Lobo, L. Vandenberghe, S. Boyd, and H. Lebret, "Applications of second-order cone programming," *Linear Algebra Appl.*, vol. 284, nos. 1–3, pp. 193–228, Nov. 1998.
[34] S. Boyd *et al.*, "Notes on decomposition methods," Stanford Univ., Stanford, CA, USA, Tech. Rep. EE364B, 2007, pp. 1–36.
[35] A. Tölli, H. Pennanen, and P. Komulainen, "Decentralized minimum power multi-cell beamforming with limited backhaul signaling," *IEEE Trans. Wireless Commun.*, vol. 10, no. 2, pp. 570–580, Feb. 2011.

ANIMESH YADAV (S'08–M'13) was a Post-Doctoral Fellow and a Research Scientist with UQAM, Canada, and CWC, University of Oulu, Finland, respectively. From 2003 to 2007, he was a Software Specialist with iGate Inc., India and Elektrobit Oy., Finland. He is currently a Post-Doctoral Fellow with Memorial University, Canada. His research interests include enabling technologies for future wireless networks and green communications. He was a recipient of the prestigious scholarship from The Fonds de Recherche du Québec-Nature et Technologies for Post-Doctoral research in 2015 and 2016, and the best paper award at the IEEE WiMOB-2016.

He received the B.E. degree (Hons.) from Dr. B. R. Ambedkar University, Agra, India, in 2001, the M.Tech. degree from IIT at Roorkee, Roorkee, India, in 2003, and the Ph.D. degree from the University of Oulu, Finland, in 2013.

OCTAVIA A. DOBRE (M'05–SM'07) received the Engineering Diploma and Ph.D. degrees from the Politehnica University of Bucharest, Romania, in 1991 and 2000, respectively. She was a recipient of a Royal Society Scholarship from Westminster University, U.K., in 2000, and held a Fulbright Fellowship with the Stevens Institute of Technology, USA, in 2001. From 2002 to 2005, she was with the Politehnica University of Bucharest and the New Jersey Institute of Technology, USA. In 2005, she joined Memorial University, Canada, where she is currently a Full Professor and the Research Chair. She was a Visiting Professor with the Université de Bretagne Occidentale, France, and the Massachusetts Institute of Technology, USA, in 2013.

She has co-authored over 190 journal and conference papers, and gave over 40 invited talks to industry and academia.

Her research interests include 5G technologies, blind signal identification and parameter estimation techniques, cognitive radio systems, and transceiver optimization algorithms for wireless communications and optical and underwater communications.

Dr. Dobre served as the General Chair of CWIT, and the Technical Co-Chair of symposia at numerous conferences, such as the IEEE GLOBECOM and the ICC. She is the Chair of the IEEE ComSoc Signal Processing for Communications and Electronics Technical Committee, the Chair of the IEEE ComSoc WICE Standing Committee, and a Member-At-Large of the Administrative Committee of the IEEE Instrumentation and Measurement Society. She serves as the Editor-in-Chief of the IEEE COMMUNICATIONS LETTERS, and an Editor of the IEEE COMMUNICATIONS SURVEYS AND TUTORIALS and the IEEE SYSTEMS. She was an Editor and a Senior Editor of the IEEE COMMUNICATIONS Letters, an Editor of the IEEE TRANSACTIONS ON WIRELESS COMMUNICATIONS, and the Guest Editor for other prestigious journals.

NIRWAN ANSARI (S'78–M'83–SM'94–F'09) is currently a Distinguished Professor of Electrical and Computer Engineering with the New Jersey Institute of Technology (NJIT). He has been also a Visiting (Chair) Professor with several universities, such as High-level Visiting Scientist with the Beijing University of Posts and Telecommunications.

He has authored the book *Green Mobile Networks: A Networking Perspective* (IEEE-Wiley, 2017) with T. Han, and co-authored two other books. He has also co-authored over 500 technical publications and over 200 published in widely cited journals/magazines. His current research interests include green communications and networking, cloud computing, and various aspects of broadband networks. He has guest-edited a number of special issues covering various emerging topics in communications and networking. He has served on the Editorial/Advisory Board of over ten journals.

He has also been granted over 30 U.S. patents. Some of his recognitions include several Excellence in Teaching Awards, a few best paper awards, the ComSoc TCGCC Distinguished Technical Achievement Recognition Award, the NCE Excellence in Research Award, the ComSoc AHSN TC Technical Recognition Award, the NJ Inventors Hall of Fame Inventor of the Year Award, the Thomas Alva Edison Patent Award, Purdue University Outstanding Electrical and Computer Engineer Award, and designation as a COMSOC Distinguished Lecturer. He was elected to serve in the IEEE Communications Society Board of Governors as a Member-At-Large. He has chaired ComSoc technical committees, and has been actively organizing numerous IEEE International Conferences/Symposia/Workshops. He has frequently been delivering keynote addresses, distinguished lectures, tutorials, and invited talks.

He received the B.S.E.E. (*summa cum laude* with a perfect GPA) degree from NJIT in 1982, the M.S.E.E. degree from the University of Michigan in 1983, and the Ph.D. degree from Purdue University in 1988.